On-Chip Integration Operating Under the Extraordinary Light Detection Mode of an InGaN/GaN Diode

Yongchao Yang, Xumin Gao, Jialei Yuan, Yuanhang Li, Zhiyu Zhang, and Yongjin Wang

***Abstract*— In this letter, we build an on-chip photonic integration system on a GaN-on-silicon platform. Using silicon removal and back wafer etching techniques, two suspended InGaN/GaN multiple-quantum-well diodes (MQWDs), which are connected by suspended waveguides, are fabricated as a transmitter and a receiver, respectively, in the on-chip photonic integration system. The 100-μm-long, 2-μm-high, and 3-μm-wide suspended waveguides are adopted for light coupling and transmission between the transmitter and the receiver. When the transmitter emits light, the InGaN/GaN MQWD simultaneously exhibits an extraordinary light detection mechanism in which the light-induced electron-hole pairs are greatly increased and can be rapidly cancelled by the injection current. The on-chip photonic integration system experimentally demonstrates the significantly improved 3-dB bandwidth and data transport performances when the receiver operates under the simultaneous light emission and detection mode.**

***Index Terms*— InGaN/GaN multiple-quantum-well diode, on-chip photonic integration, light detection and emission.**

I. Introduction

THE GaN-on-silicon platform is promising for use in on-chip optical interconnects, in which the emitter, waveguide and detector are integrated on a single chip [1]–[4]. A compact fluorescence analysis system was demonstrated by monolithically integrating GaN blue light-emitting diode (LED), silicon photodiode and polydimethylsiloxane micro-channels on a silicon substrate [5]. The on-chip photonic integration of light source, waveguide and photodiode provides new opportunities to use the high-speed optical pumping or detection for bio sample on a silicon single chip [6]. InGaN/GaN multiple-quantum-well diodes (MQWDs) can be used as either LEDs to emit light or photodiodes to detect light [7], [8]. Hence, on the basis of InGaN/GaN MQWDs, both emitters and detectors can be produced on the same substrate using the same fabrication processes. The emission and detection wavelengths are controllable by tuning the indium content in the InGaN/GaN MQWDs [9]–[11]. Theoretically, when the InGaN/GaN MQWDs are turned on to emit light, they still can detect the incident light and generate light-induced electron-hole pairs. Therefore, they exhibit an extraordinary light detection mechanism, which is of great interest for building a portable biological sensor platform or on-chip photonic integration system on a single chip. GaN has a low transmission loss in the visible light region [12]–[15]. However, silicon has a higher refractive index than that of GaN and absorbs visible light. Therefore, a highly confined suspended waveguide, which is probable for light coupling and transmission to achieve an optical interconnect between transmitter and detector, is thus fabricated via a combination of silicon removal and back wafer etching. The silicon absorption of visible light is also eliminated.

Here, we demonstrate a wafer-level process for the fabrication of the on-chip photonic integration system on a single chip [16]–[18]. Both silicon removal and back-side thinning are conducted to achieve suspended device architectures. The InGaN/GaN MQWDs are adopted as the transmitter and the receiver, respectively, in the on-chip photonic integration system. The light detection mechanisms of the InGaN/GaN MQWDs are investigated in detail, and the light coupling and transmission through suspended waveguides are experimentally demonstrated. The wire-bonded chip exhibits the bias-voltage-dependent 3-dB bandwidth and data transmission performances of the on-chip photonic integration system.

II. Experimental Results and Discussion

The on-chip photonic integration system is implemented on a 2-inch GaN-on-silicon wafer. The top epitaxial layers consist of an 80-nm-thick p-GaN layer, a 35-nm-thick p-AlGaN layer, a 120-nm-thick layer of InGaN/GaN MQWDs, a 3400-nm-thick n-GaN layer, a 400-nm-thick undoped GaN layer, a 600-nm-thick AlGaN buffer layer, and a 330-nm-thick AlN layer. The total thickness is approximately 5 μm. Hence, a doubled-side process is used to remove the silicon substrate and to etch a suspended membrane on the backside, leading to a highly confined optical waveguide for guiding light. The chip is 0.8 cm$\times$0.8 cm and is separated from the processed wafer, which is wire-bonded to a test pad for device characterization, as shown in Fig. 1(a). As a light-emitting diode, the InGaN/GaN MQWD emits light in all directions when it is turned on. The guided modes

Manuscript received November 18, 2016; revised December 26, 2016; accepted January 16, 2017. Date of publication January 20, 2017; date of current version February 10, 2017. This work was supported in part by Research Projects under Grant S2016G6424 and Grant BE2016186, in part by the National Natural Science Foundation of China under Grant 61322112 and Grant 61531166004, and in part by the Innovative Cross-disciplinary Team Program of CAS.

Y. Yang, X. Gao, J. Yuan, Y. Li, and Y. Wang are with the Grünberg Research Centre, Nanjing University of Posts and Telecommunications, Nanjing 210003, China (e-mail: wangyj@njupt.edu.cn).

Z. Zhang is with the Changchun Institute of Optics, Fine Mechanics and Physics, Chinese Academy of Science, Changchun 130033, China (e-mail: zhangzhiyu@ciomp.ac.cn).

Color versions of one or more of the figures in this letter are available online at http://ieeexplore.ieee.org.

Digital Object Identifier 10.1109/LPT.2017.2655566

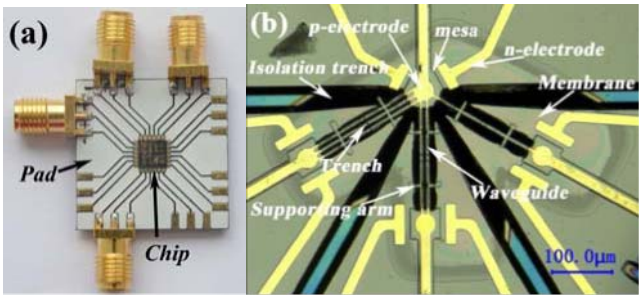

Fig. 1. (a) The wire-bonded chip; (b) Optical microscope image of the fabricated on-chip photonic integration system.

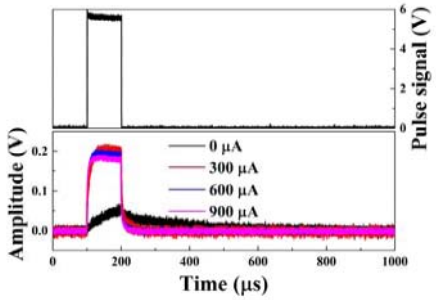

Fig. 2. The decay characteristics of the on-chip photonic integration system versus the injection currents.

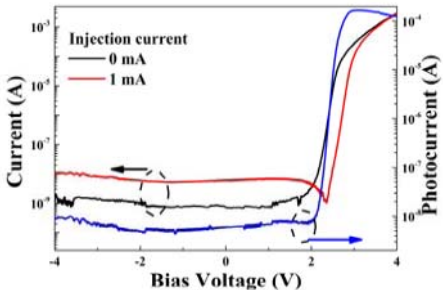

Fig. 3. The log-scaled I-V and induced photocurrent plots for the receiver.

may be coupled into the suspended waveguides parallel to the wafer surface. The light is then guided by the highly confined suspended waveguides after the silicon substrate is removed, followed by back wafer etching. Recently, Sun *et al.* demonstrated room-temperature continuous-wave electrically injected InGaN-based laser grown on silicon substrate [19], which can increase the coupling efficiency between light source output and waveguide. Alternatively, the InGaN/GaN MQWD can used as a photodiode to detect the light and complete the photon-electron conversion. Figure 1(b) shows an optical microscope image of the fabricated 1×3 on-chip photonic integration system. Both transmitters and receivers have a p-electrode with 18 μm in diameter, which is connected to an electrode wire bonding pad. The device capacitance can be decreased by reducing the size of electrode, leading to an improved bandwidth of the LEDs. Nanowire array InGaN/GaN LEDs demonstrated an on-off keying device operation over 1 Gbps [20]. Except for the bonding pads, the transmitter, waveguide and receiver are fabricated on the suspended membrane. Waveguides with smaller width can effectively reduce the confined optical modes and thus improve the transmission rate. From the fabrication point of view, waveguides with smaller width are fragile and can easily break during silicon removal and backside thinning processes. Hence, the 3-μm-wide supporting arms are used to manage the fracturing of 100-μm-long, 2-μm-high and 3-μm-wide suspended waveguides. In the middle of the waveguide, both p-GaN and InGaN/GaN MQWs layers are removed to form a 3-μm-wide trench, resulting in separation in the p-GaN layers for the transmitter and the receiver.

The decay characteristics of the on-chip photonic integration system are characterized using the pulse measurements by a combination of a Keysight 81160A pulse function arbitrary generator, an Agilent DSO9254A digital storage oscilloscope and an Agilent B1500A semiconductor device analyzer. For the wire-boned on-chip photonic integration chip, the pulse signal is applied to the transmitter, leading to a pulsed light emission. The receiver absorbs the guided light by suspended waveguides and then converts photons into electrons. The signals are then recorded by the oscilloscope. Moreover, the driven currents are injected into the receiver by the semiconductor device analyzer, which enables the receiver to sense the incoming light and emit light at the same time. Figure 2 shows the decay curves versus the injection currents when a 100 μs pulse signal is applied on the transmitter. When the injection current is 0 μA, it is obvious that the received signal increases and reaches the maximum value when the pulse signal is finished and gradually returns to the initial state. As the receiver is driven by the injection current, the device barrier is managed, and thus the absorbed light can generate many more electron-hole pairs. The decay time becomes shorter when the injection currents are increased from 300 μA to 900 μA because the induced photocurrents can be cancelled by the injection currents. Therefore, the received signals are rapidly saturated and decay quickly when the pulse signals are finished.

The light emission intensity at the transmitter is dependent on the injection current [21]–[23], and the induced photocurrent at the receiver is influenced by the absorbed light. Hence, the current-voltage (I-V) performance at the receiver can be tuned by the injection current at the transmitter. Figure 3 shows the log-scaled I-V plots for the receiver. The sharp dip occurring at approximately 2.36 V indicates that the induced photocurrent is equal to the driven current at the receiver. The induced photocurrents are obtained by subtracting measured current values at the injection current of 1 mA using the measured current values at the injection current of 0 mA for the transmitter. It is obvious that the I-V plots of the receiver are tuned by the injection currents of the transmitter, and the receiver exhibits dual light detection modes. When InGaN/GaN MQWD operates under the light emission and detection mode, it emits and detects light simultaneously, indicating that both light emission and detection occur when the forward bias is higher than the turn-on voltage. The light generates electron-hole pairs inside the MQW active layers due to the piezo-field effect [24]. This special phenomenon is promising for a full-duplex data transmission using visible

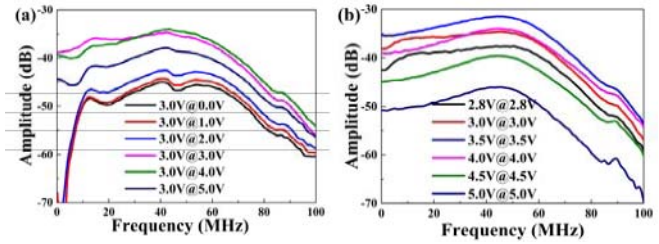

Fig. 4. (a) The measured S_{21} parameter versus the applied voltage of the receiver; (b) Voltage-dependent S_{21} behavior.

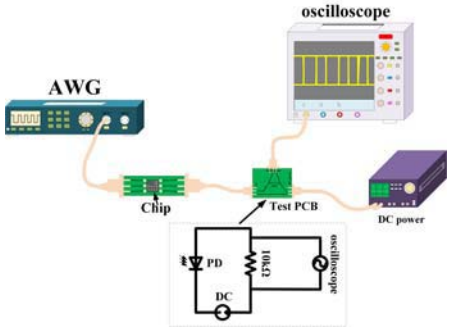

Fig. 5. Schematic of the experimental setup.

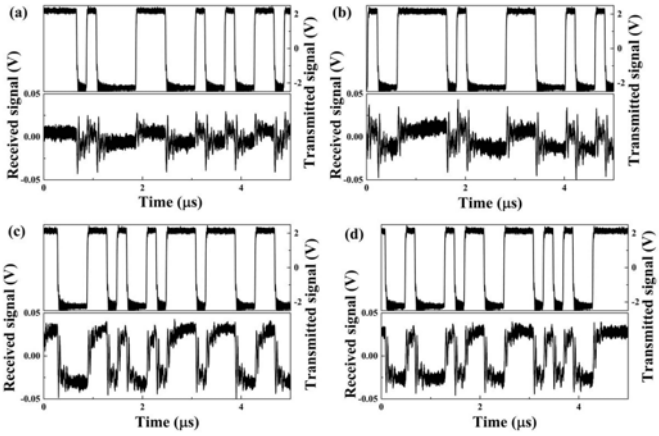

Fig. 6. PRBS data transmission: (a) 0 V; (b) 3.0 V; (c) 5.0 V; (d) 6.0 V.

light, leading to an improved channel capacity. According to Fig. 3, both light detection and emission are dependent on the forward bias with different mechanisms and thus, the optimum forward bias for light detection and emission would be different.

Using a Keysight ENA network analyzer E5080A and Rigol DP832 DC power supply, the full two-port measurements are conducted to further investigate the proposed on-chip photonic integration system. When the transmitter is driven by a DC power with 3.0 V, the applied voltage to the receiver varies. The transmission frequency response S_{21} parameter refers to the signal exiting at port 2 for the signal incident at port 1. Figure 4(a) shows the measured S_{21} parameter versus the applied voltage of the receiver. The S_{21} performance is slightly improved with increasing the voltage from 0 to 2.0 V, in which the receiver is turn-off and operates under light detection mode. As the applied voltage is 3.0 V, the receiver is turned on and the S_{21} performance is thus greatly improved. The on-chip photonic integration system exhibits a 3-dB bandwidth of approximately 63 MHz at the voltages of 3.0 V@3.0 V. Subsequently, the S_{21} performance is slightly decreased with increasing the voltage from 3.0 to 5.0 V, indicating that there is a trade-off between the bias voltage at the transmitter and the applied voltage at the receiver. Therefore, equal voltages are applied on the transmitter and the receiver, as shown in Fig. 4(b). The S_{21} performance is continuously improved with increasing the voltages 2.8 V@2.8 V to 3.5 V@3.5 V; however, the performance is decreased with further increase in the voltages up to 5.0 V@5.0 V. A 3-dB bandwidth of approximately 70 MHz is achieved at the voltages of 3.5 V@3.5 V for the on-chip photonic integration system. These results are in good agreement with the I-V plots, suggesting that the on-chip photonic integration system can achieve higher performance when the induced photocurrent is comparable to the injection current at the receiver.

As demonstrated in Fig. 5, on the transmitter side, the InGaN/GaN MQWD is directly driven by an Agilent 33522A arbitrary waveform generator to output the modulated light. On the receiver side, another MQWD is connected to a load resistance and a power source in series, and the signals at the 10 kΩ load resistance is characterized by an Agilent DSO9254A digital storage oscilloscope without amplification. Electron-photon conversion and photon-electron conversion occur at the transmitter and the receiver, respectively, to achieve in-plane communication using visible light. Pseudo-random binary sequence (PRBS) data are transmitted at 5 Mbps, and Figure 6 shows the received PRBS data versus the applied voltage at the receiver side. The receiver is turned off and serves as a photodiode when the applied voltage is 0.0 V. As shown in Fig. 6 (a), the amplitudes of the received signals are weak. With increasing applied voltage up to 3.0 V, the receiver is turned on and can emit and detect light at the same time. Correspondingly, the amplitudes of the received signals are slightly increased. The received PRBS data are clearly significantly improved when the applied voltages are increased to 5.0 V and 6.0 V, as shown in Figs. 6(c) and 6(d), respectively. The eye diagrams are measured at 5 Mbps for evaluating the on-chip photonic integration system. Figure 7(a) illustrates the measured eye diagrams at the applied voltage of 0.0 V, in which the eyes are closed. When the applied voltage is increased to 3.0 V, the diagrams tend to show open eyes, as illustrated in Fig. 7(b). The open eyes are clearly shown and greatly improved when the applied voltages are increased to 5.0 V and 6.0 V, as illustrated in Figs. 7(c) and 7(d), respectively. These results experimentally demonstrate the voltage-dependent communication performance for the proposed on-chip photonic integration system, indicating that the improved communication ability can be obtained when the receiver operates under a simultaneous light emission and detection mode. A number of nanoscaled photonic integration using visible light has been proposed and the data transmission rate can be further improved [25].

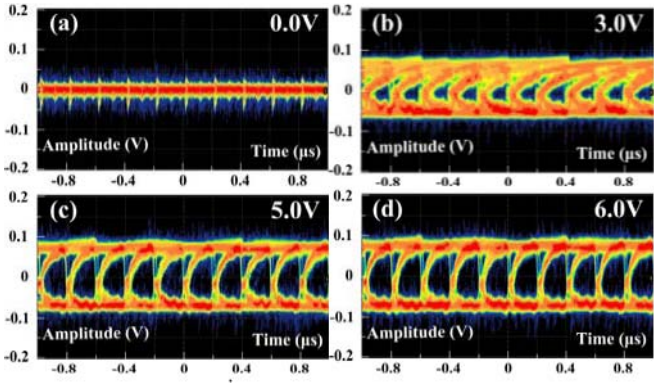

Fig. 7. Measured eye diagrams: (a) 0 V; (b) 3.0 V; (c) 5.0 V; (d) 6.0 V.

III. Conclusion

In conclusion, an on-chip photonic integration system is built on a GaN-on-silicon platform. One suspended InGaN/GaN MQWD is used as the transmitter to emit the modulated light, which is coupled into the suspended waveguide and propagates to the receiver. Another InGaN/GaN MQWD that acts as the receiver absorbs the modulated light and converts photons into electrical signals, leading to the in-plane data transport using visible light. Pulse test, I-V characterization, 3-dB bandwidth, PRBS and eye diagram measurements were conducted to evaluate the fabricated on-chip photonic integration system. The results experimentally demonstrated that the InGaN/GaN MQWD exhibits an extraordinary light detection mechanism while emitting light at the same time, and the 3-dB bandwidth and data transport performances for the on-chip photonic integration system are greatly improved when the receiver operates under a simultaneous light emission and detection mode.

References

[1] M. D. Brubaker *et al.*, "On-chip optical interconnects made with gallium nitride nanowires," *Nano Lett.*, vol. 13, no. 2, pp. 374–377, 2013.

[2] M. Tchernycheva *et al.*, "Integrated photonic platform based on InGaN/GaN nanowire emitters and detectors," *Nano Lett.*, vol. 14, no. 6, pp. 3515–3520, Jun. 2014.

[3] Z. Jiang *et al.*, "Monolithic integration of nitride light emitting diodes and photodetectors for bi-directional optical communication," *Opt. Lett.*, vol. 39, no. 19, pp. 5657–5660, 2014.

[4] T. Sato *et al.*, "Photonic crystal lasers for chip-to-chip and on-chip optical interconnects," *IEEE J. Sel. Topics Quantum Electron.*, vol. 21, no. 6, Nov./Dec. 2015, Art. no. 4900410.

[5] H. Nakazato, H. Kawaguchi, A. Iwabuchi, and K. Hane, "Micro fluorescent analysis system integrating GaN-light-emitting-diode on a silicon platform," *Lab Chip*, vol. 12, no. 18, pp. 3419–3425, 2012.

[6] R. M. Vazquez *et al.*, "Integration of femtosecond laser written optical waveguides in a lab-on-chip," *Lab Chip*, vol. 9, no. 1, pp. 91–96, 2009.

[7] P. Dietz, W. Yerazunis, and D. Leigh, "Very low-cost sensing and communication using bidirectional LEDs," in *UbiComp 2003: Ubiquitous Computing* (Lecture Notes in Computer Science), vol. 2864, A. Dey, A. Schmidt, and J. McCarthy, Eds. Berlin, Germany: Springer, 2003, pp. 175–191. [Online]. Available: http://dx.doi.org/10.1007/978-3-540-39653-6 14

[8] X. Li *et al.*, "Suspended p–n junction InGaN/GaN multiple-quantum-well device with selectable functionality," *IEEE Photon. J.*, vol. 7, no. 6, Dec. 2015, Art. no. 2701407.

[9] T. Kuykendall, P. Ulrich, S. Aloni, and P. D. Yang, "Complete composition tunability of InGaN nanowires using a combinatorial approach," *Nature Mater.*, vol. 6, pp. 951–956, Oct. 2007.

[10] F. Qian *et al.*, "Multi-quantum-well nanowire heterostructures for wavelength-controlled lasers," *Nature Mater.*, vol. 7, pp. 701–706, Aug. 2008.

[11] R. Chen *et al.*, "Nanolasers grown on silicon," *Nature Photon.*, vol. 5, pp. 170–175, Feb. 2011.

[12] Y. Zhang *et al.*, "GaN directional couplers for integrated quantum photonics," *Appl. Phys. Lett.*, vol. 99, no. 16, p. 161119, 2011.

[13] N. V. Triviño, U. Dharanipathy, J.-F. Carlin, Z. Diao, R. Houdré, and N. Grandjean, "Integrated photonics on silicon with wide bandgap GaN semiconductor," *Appl. Phys. Lett*, vol. 102, no. 8, p. 081120, 2013.

[14] S. Shokhovets, M. Himmerlich, L. Kirste, J. H. Leach, and S. Krischok, "Birefringence and refractive indices of wurtzite GaN in the transparency range," *Appl. Phys. Lett.*, vol. 107, no. 9, p. 092104, 2015.

[15] T. Sekiya, T. Sasaki, and K. Hane, "Design, fabrication, and optical characteristics of freestanding GaN waveguides on silicon substrate," *J. Vac. Sci. Technol. B, Microelectron. Process. Phenom.*, vol. 33, no. 3, p. 031207, 2015.

[16] W. Cai *et al.*, "Integrated p-n junction InGaN/GaN multiple-quantum-well devices with diverse functionalities," *Appl. Phys. Exp.*, vol. 9, no. 5, p. 052204, 2016.

[17] Y. Wang *et al.*, "On-chip photonic system using suspended p-n junction InGaN/GaN multiple quantum wells device and multiple waveguides," *Appl. Phys. Lett.*, vol. 108, no. 16, p. 162102, 2016.

[18] W. Cai *et al.*, "On-chip integration of suspended InGaN/GaN multiple-quantum-well devices with versatile functionalities," *Opt. Exp.*, vol. 24, no. 6, pp. 6004–6010, 2016.

[19] Y. Sun *et al.*, "Room-temperature continuous-wave electrically injected InGaN-based laser directly grown on Si," *Nature Photon.*, vol. 10, no. 9, pp. 595–599, 2016.

[20] R. Koester *et al.*, "High-speed GaN/GaInN nanowire array light-emitting diode on silicon(111)," *Nano Lett.*, vol. 15, no. 4, pp. 2318–2323, 2015.

[21] J. Vučić, C. Kottke, S. Nerreter, K. D. Langer, and J. W. Walewski, "513 Mbit/s visible light communications link based on DMT-modulation of a white LED," *J. Lightw. Technol.*, vol. 28, no. 24, pp. 3512–3518, Dec. 15, 2010.

[22] J. J. D. McKendry *et al.*, "Visible-light communications using a CMOS-controlled micro-light-emitting-diode array," *J. Lightw. Technol.*, vol. 30, no. 1, pp. 61–67, Jan. 1, 2012.

[23] C.-L. Liao, C.-L. Ho, Y.-F. Chang, C.-H. Wu, and M.-C. Wu, "High-speed light-emitting diodes emitting at 500 nm with 463-MHz modulation bandwidth," *IEEE Electron Device Lett.*, vol. 35, no. 5, pp. 563–565, May 2014.

[24] B. J. Van Zeghbroeck, C. Harder, H. P. Meier, and W. Walter, "Photon transport transistor," in *IEDM Tech. Dig.*, 1989, pp. 543–546.

[25] M. S. Islam and V. J. Logeeswaran, "Nanoscale materials and devices for future communication networks," *IEEE Commun. Mag.*, vol. 48, no. 6, pp. 112–120, Jun. 2010.